

Impact on timing and light extraction of a photonic crystal as measured on a half patterned LYSO crystal: implications for time of flight PET imaging

To cite this article: A. Iltis *et al* / 2019 *JINST* **14** P06036

View the [article online](#) for updates and enhancements.



IOP | ebooks™

Bringing you innovative digital publishing with leading voices to create your essential collection of books in STEM research.

Start exploring the collection - download the first chapter of every title for free.

Impact on timing and light extraction of a photonic crystal as measured on a half patterned LYSO crystal: implications for time of flight PET imaging

A. Iltis,^{a,b,1} S. Zanettini,^a L.R. de Magalhaes,^b C. Tata,^b A. Soledade,^b M.Z. Hmissi,^c H. Khadiri,^d V. Gaté^d and D. Turover^a

^aNapa Technologies, 10000 Troyes, France

^bDamavan Imaging, 10430 Rosières près Troyes, France

^cUniversity of Technologies of Troyes, 10300 Troyes, France

^dSilsef, 77140 Archamps, France

E-mail: alain.iltis@damavan-imaging.com

ABSTRACT: The improvement of the energy and of the timing resolution is always a challenge in scintillation-based detectors. A large fraction of the photons produced by scintillation remains trapped inside the crystal. Photonic crystals have been suggested as a solution to improve light extraction. Here we will present results obtained with a nanostructured TiO₂ coating on a 50 × 50 mm² LYSO crystal. The objective of the present paper is to characterize the performance of this coating in both light extraction and timing performance as both parameters are critical to spatial resolution of PET systems. To avoid tricky calibration problems, especially for timing, we have manufactured a monolithic crystal with one half patterned with a photonic crystal and with one half bare. We are rotating the crystal $\pi/2$ relative to the photo-detector between each measure. We have chosen a digital Si-PM Philips DPC 3200 as photo-detector due to its excellent timing precision and stability. The impact on light extraction of the photonic crystal is very strong as 30% of the light only escaped through the naked face vs 70% through the textured face for each position. The timing effect is much more subtle and quite at odd with previous results. By averaging the measurements on four positions, we are detecting a time lag effect of photon extraction with a probability of 98%. The average lag is only of 17 ps on the detection in the textured part of the crystal. This effect, although without practical consequences for PET imaging, is nevertheless perplexing as we were foreseeing a faster exit of photons on the textured face. We propose an explanation for the effect observed.

KEYWORDS: Gamma detectors (scintillators, CZT, HPG, HgI etc); Instrumentation and methods for time-of-flight (TOF) spectroscopy; Photon detectors for UV, visible and IR photons (solid-state) (PIN diodes, APDs, Si-PMTs, G-APDs, CCDs, EBCCDs, EMCCDs, CMOS imagers, etc); Timing detectors

¹Corresponding author.

Contents

1	Introduction	1
2	Materials and methods	2
2.1	The half patterned crystal	2
2.2	Philips DPC 32000 digital Si-PM	3
2.3	Experimental set-up	4
3	Results and discussion	5
3.1	Light extraction efficiency	5
3.2	Timing calibration and timing data matrix construction	6
3.3	Photon timing data analysis	8
3.4	Possible Interpretation of the slight delay related to the texturing	9
4	Conclusions	10

1 Introduction

The improvement of light yield and of the timing resolution is always a challenge in scintillation-based detectors in the context of PET scanners, as both parameters are directly correlated with spatial resolution and signal/noise ratio. Both parameters are linked to the number of photons successfully collected by the photodetectors. Most of the scintillators with high light yields suffer from a high refractive index, resulting in a poor light extraction efficiency. A large fraction of the scintillation photons produced remains trapped inside the crystal due to total internal reflection (TIR). Photonic crystals have been initially suggested for light extraction enhancement in light emitting diodes since they inhibit spontaneous in-plane emission [1, 2]. Later, they have been proposed as a solution to improve light extraction on high index scintillating crystals by using them as efficient diffraction gratings [3–5]. The role of a photonic crystal coating on the surface of an inorganic scintillator is to out-diffract the photons impinging the exit surface beyond the critical angle into diffraction orders (other than zero-th order), thus increasing the light extraction efficiency and the total amount of light collected by the photo-sensor [6].

So far they have found limited application due to the difficulty in manufacturing these nano-structures on a large surface with a sufficient optical quality. Nano-imprint has been proposed as a way to manufacture such structures on size larger than 2 inches [7].

Here we will present results obtained with a TiO_2 coating obtained by nano-imprint on a 50×50 mm² exit surface of a LYSO crystal: the pattern has a periodicity of 1000 nm and featured cones of 560 nm height and 300 nm basal diameter. The objective of the present paper is to characterize the performance of this coating in both light extraction and timing performance. The classical method is to measure the crystal before and after patterning with the same set-up. But in that

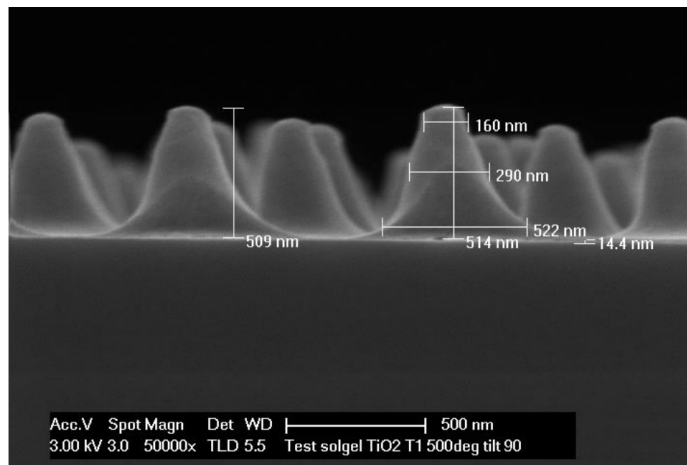


Figure 1. SEM image of Nano-pattern.

case, the calibration is tricky specially for timing measurements as the performance of the Si-PM is dependent on many parameters like temperature, Vbias, optical path, etc. . . We are also looking for a very slight timing effects < 100 ps. It appears difficult to measure such a slight difference in timing in different acquisition runs and while you need to dismantle and reassemble the setup.

For this reason, we have manufactured a monolithic crystal with one half nano-patterned with a photonic crystal and one half bare. Our target is to characterize this half patterned crystal using the same photo-detector on the same observing run. We were doing four measures by rotating the crystal relative to the photo-detector. All the acquisitions were done the same day. This allows to avoid detector inhomogeneity and calibration issues. If the effect observed is real, it should be visible for all rotation position of the crystal. We have chosen to use a digital Si-PM Philips DPC 3200 as the photo-detector due to its excellent timing and stability [8].

2 Materials and methods

2.1 The half patterned crystal

The LYSO crystal is a square truncated pyramid with a 50×50 mm² square base truncated from its top. The top face is 40×40 mm² (entry face) and the thickness is 10 mm.

The upper surface is polished. The lateral faces and lower surface are roughened so as to ensure a scattering return. The 50×50 mm² face is the exit face we are measuring. Lateral and entry faces are covered by Teflon tape to ensure diffusive return and good photon collection efficiency. Half of the 50×50 mm² exit surface has been textured with a sol-gel TiO₂ coating recrystallized to get a high index ($n = 2.15$). The pattern has a periodicity of 1000 nm and featured cones of 560 nm height and 300 nm basal diameter as shown in figure 1.

The patterned half-surface is clearly apparent as grayish to the eyes as it can be seen in the image below (figure 2). The coating appears homogeneous in glancing light.

In order to avoid spoiling the coating during handling, an air coupling with a gap thickness of 300 microns was chosen between the crystal and the photo-detector. The refractive index gap was thus between LYSO ($n = 1.83$) and air ($n = 1$).



Figure 2. Image of the half patterned LYSO crystal.

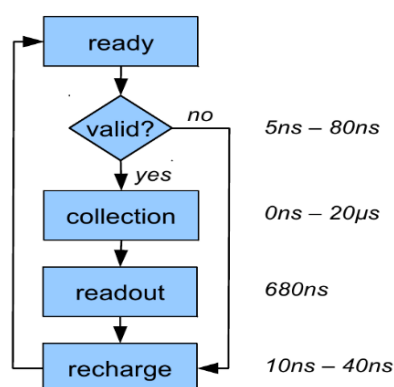


Figure 3. Philips DPC acquisition logic.

2.2 Philips DPC 32000 digital Si-PM

The DPC-3200-22 sensor consists of 16 independent die sensors arranged in a 4×4 array. A die sensor contains four pixels, arranged in a 2×2 array, and each pixel consists of 3200 SPAD cells [8]. The size of each SPAD cell is $59.4 \times 64 \mu\text{m}^2$. The dimension of each die is $7.15 \times 7.8775 \text{ mm}^2$ and each pixel of a die has an area of $3.2 \times 3.8775 \text{ mm}^2$. Thus the effective area covered by the detector is $32 \times 32 \text{ mm}^2$. A pair of time to digital converters (TDCs) coupled to each die generates a single time stamp. The phase difference between the two TDC allows an error correction on time-stamps [8]. The timestamp generation is determined by the configured trigger threshold, which can be set to the level of the first photon or, alternatively, to higher photon thresholds. We choose to use first photon trigger level during our measurements, in order to get the best timing performance. The figure 3 shows the acquisition logic of Philips DPC. More detailed information could be obtained in ref. [8].

Once an event is detected above the trigger, the system waits for a duration that can be set between 5 ns and 80 ns for validation. Then the duration of acquisition can be set between 0 ns and 20 μs . Finally, the chip is readout during 680 ns and goes to recharge for 10–40 ns.

As we have told before, our trigger level is the lowest possible (1 photon) on each pixel in order to get the first photons from each interaction. If enough photons are detected during the experiment validation interval, the event is considered as valid. So an event may be valid with only one pixel seeing one photon.

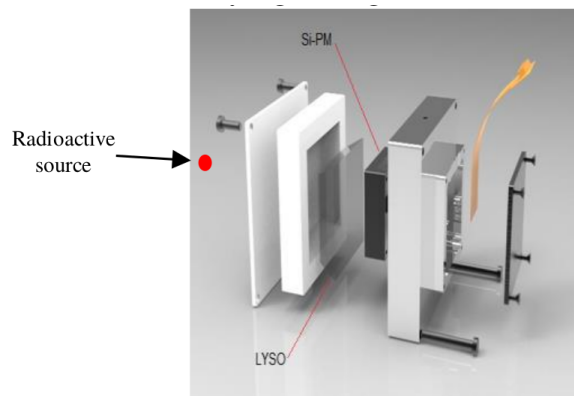


Figure 4. Experimental set-up for measuring the half patterned crystal.

Once an event is validated at the die level, the Philips system records the time when the first photon was detected and the energy deposited on each pixel of the die during the integration time (620 ns). In our experiment, all dies are independent. If a die event is validated, the neighbour die may not. We then discard all the events whose energy is below 100 photons in order to get rid of electronic noise.

At the end of the measurement we get a file giving for each validated event, the reference of the die activated, the number of photons detected by the die, the time stamp of the first photon detected by the die and the SiPM tile temperature. We call that file a matrix of event. This matrix of event contains both the photon distribution for each 64 pixels and the time of arrival distribution for each of the 16 dies. We'll study both parameters in this article. Section may be divided by subheadings. It should provide a concise and precise description of the experimental results, their interpretation as well as the experimental conclusions that can be drawn.

2.3 Experimental set-up

The crystal is larger than the detector in order to limit edges effects. Photons are lost along the edges of the crystal resulting in a lower number of photons detected close to those edges. The histogram of the number of photon collected as a function of distance from the center shows a curvature towards the edges. Edge effects also affects the timing measurements. In order to limit those problems, we have chosen to observe only the central part of the crystal. Light and timing distribution there have only a weak curvature as seen by the photodetector. As the crystal ($50 \times 50 \text{ mm}^2$) is larger than the detector ($32 \times 32 \text{ mm}^2$), we have designed a special set-up to center the crystal on the detector and avoid stray light (figure 4).

The detection device is the Philips Digital Photon Counting Tile-TEK. The Si-PM tile is maintained centered in front of the large base of the crystal thanks to the housings (figure 4). The crystal and the Si-PM are not in contact since the housings maintain a $300 \mu\text{m}$ air gap between them. The source is a $0.53 \text{ MBq } ^{22}\text{Na}$ centered along the symmetry axis of the setup. The distance between the source and the entry face of the crystal is 20 cm.

In this set-up, the light collected on the edge of the crystal is lost because the crystal exit surface is larger than the detector. Thus, it is difficult to get a good energy resolution measurement. We have nevertheless observed a peak in the number of photons detected between 500 and 1000

photons. This peak corresponds in our set-up to the 511 keV peak emitted by ^{22}Na in monolithic LYSO in configuration where mostly undiffused photons are recorded. We have thus selected the events detected between 500 and 1000 photons. The acquisition duration was 1000s. The total number of valid events is recorded in table 1 and varies between 169440 and 194908 events.

The measurement is carried on inside a controlled temperature chamber to prevent temperature variation during the acquisition. The tile temperature is monitored during the acquisition. The measurement was performed for a SiPM tile temperature of 10°C .

3 Results and discussion

3.1 Light extraction efficiency

For each valid event, the DPC acquires the full light distribution in term of number of photons/pixels. Our goal is to investigate the impact of patterning on average light extraction efficiency. With our set-up, the flux of gamma photons is nearly uniform across the field of view of the detector. Hence, the probability of a scintillation event is also quasi constant across the field of view of the detector. We are close to an isotropic distribution of events. We are rotating the crystal by $\pi/2$ while keeping the photo-detector fixed between each acquisition. The patterns observed in the light and time distribution, if linked to the pattern on the crystal and not to photo-detector, should thus rotate of $\pi/2$ between the acquisitions.

We have decided to make the sum of the light distribution on each half of the crystal of all the valid events. In this way an enhanced extraction efficiency from part of the crystal exit face would translate in a higher number of photons detected there. We have thus added the number of photons detected by each pixel for all the 180000 or so valid interactions. We have then calculated the average contribution of each pixel in percent to the total number of photons detected in the sum of all valid events. This value in percent is written on each pixel and a color code has also been given to the pixels. The sum of all 64 pixels gives 100.

When we have done this experiment with un-textured crystals we have effectively observed quite flat response along the $32 \times 32 \text{ mm}^2$ field of view. In order to avoid tile light output calibration issues four acquisitions were done with the crystal rotated by $\pi/2$ between each acquisition. All acquisitions were done in the same day with a time window of 30 min between two successive rotations.

The enhanced light extraction on the patterned part is clearly visible in figure 5. The figure for each pixel, gives its contribution to the total light extracted on all scintillation events: 2.49 means this pixel has contributed 2.49% of the total light detected on the sum of all events.

The curvature of the light distribution can be estimated by looking at pixels light contribution value going from 2.49% in the centre to 1.90% in the edges.

We have then made an average for each crystal half (textured vs naked) of the percent of detected photons in order to compare the relative extraction efficiency of textured vs naked half.

The table 1 shows the average per-cent of the scintillation light extracted through the textured and the un-textured half of the crystal. The result is very stable around 30% for the naked face and 70% for the textured one. This would suggest that the light extraction efficiency is about twice for the textured face. Extraction yield with photonic crystal is highly dependent on the shape of the crystal and on reflectivity of lateral and upper faces. Besides, here we are only observing the central region of the crystal and the edge are not observed. Hence, the average efficiency of the coating on the whole crystal will be lower when measured on a fully textured crystal.

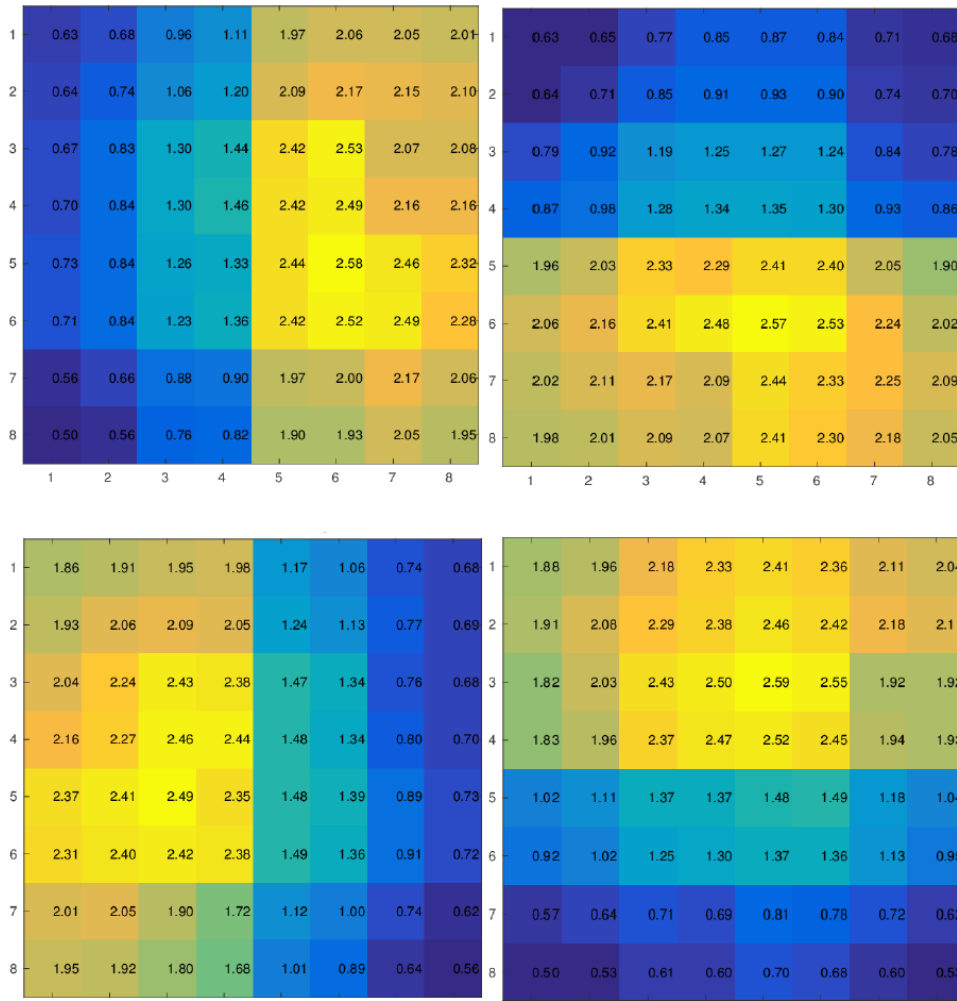


Figure 5. Average photon extraction (% of total light distribution)/pixel for a half pattern crystal rotated by $\pi/2$ steps.

Table 1. Results of various geometries in term of number of photons and in % of total light distribution for the two halves.

	<i>Number of events</i>	<i>Naked</i>	<i>Textured</i>
Textured right	194908	29.7	70.45
Textured left	185546	31.6	68.45
Textured bottom	178498	29.5	70.43
Textured up	169440	29.65	70.33

3.2 Timing calibration and timing data matrix construction

For each valid event, we are recording the time distribution of the first photons detected for each die (group of four pixels) in the event. This distribution allows us to estimate the location of the cone of un-diffused photons. The lowest time stamp recorded is set as time 0 for this event. Then we calculate for each die (n) that was observed in this event the delay dt between time stamp of die

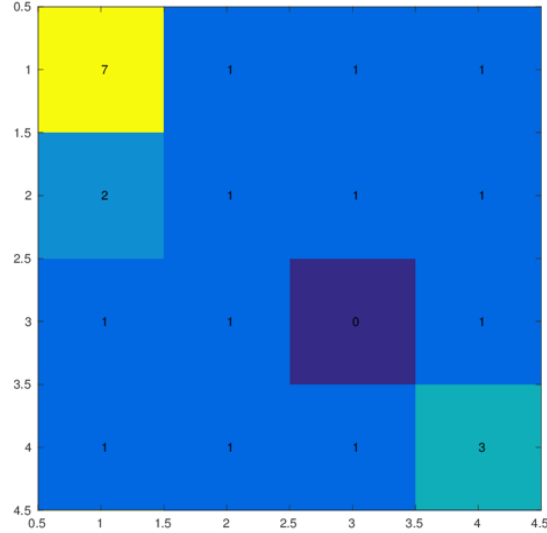


Figure 6. Residual delays die to die on a 1000 s acquisitions after timing skew correction (timing differences are in 19.5 ps unit).

n and time 0: $dt = \text{time}(n) - \text{time}(0)$. This delay is expressed in DPC time stamp unit i.e. unit of 19.5 ps. The light and time distribution are then plotted in a matrix of event.

In the raw data, there are some fixed skew related to signal propagation delays in the SiPM. This skew is a characteristic of acquisition circuit and doesn't change from an experiment to another [8]. Some dies can be as much as 46 time-stamps units behind the fastest die. To correct this skew, we established a time correction map. This correction map is a matrix 4×4 which is subtracted to the time matrix of each valid event.

This skew correction between dies is done according to published procedures [9]. The acquisition system only records the first photons to strike a die for each event. Most of the time stamps measured in the first nanosecond after a scintillation event come from un-diffused photons traveling in straight line from the scintillation event to the photo-detector [10]. Thus the “time stamp map” we build that way will be mostly a map of un-diffused photon detection, i.e. of photons extracted with a direct optical path.

To build the image below (figure 6), we have first corrected timing for fixed delays using an un-textured LYSO crystal $40 \times 40 \times 10 \text{ mm}^3$ (centered on the $32 \times 32 \text{ mm}^2$ detector using the same set-up). Then, in order to control the success of our correction procedure, using again the un-textured LYSO crystal $40 \times 40 \times 10 \text{ mm}^3$, we have averaged for each die, the residual delays in 19.5 ps time stamp unit for an acquisition duration of 1000 s. Figure 6 is thus a delay image of our system after time correction. As you can see the field image is very flat, meaning the fluctuation observed after proper timing calibration of the detector are very low. The average delay on the full tile is 1.5 units, or 29.25 ps. The maximum delay is 7 units or 136.5 ps. The standard deviation is 1.6 units or 31.2 ps.

In the Philips digital Si-PM, as explained in section 2.2, the granularity for measuring light distribution is 8×8 or 64 pixels. The granularity for the measure of time is only 4×4 or 16 pixels. Each “time pixel” or die is a group of four “light pixels”.

This figure allows us to estimate the average timing error we are doing on the two millions of events of the scintillation recorded in 1000 s acquisition time. Any change on the light propagation between the emission of light by scintillation and its direct detection translates in a skew in this “timing error” image. For example, if we observe the chamfered edge of the crystal, we see very clearly the faster timing along the edges brought by shorter average optical light path.

3.3 Photon timing data analysis

A lot of work has been published on the enhancement of light extraction that could be brought by photonic crystals in a scintillator. Little experimental results have been published on their effect on timing, although this parameter is very important for Time of Flight PET systems.

Our goal in those measurements has been to observe timing effects on a crystal with the same acquisition chain and parameters, and with minimal modifications to our set-up. Here with a partly patterned crystal there is only one photo-detector, well calibrated and one acquisition system. The modification done to the system between measurements is minimal: we just rotate the crystal by $\pi/2$, while retaining precisely the same crystal/detector relative position. For each of the previous measurements, we have measured maps of the residual delays for each die after time skew correction, built as explained in paragraph 3.2. Any effect from texturation should distort the time skew map. We have thus acquired time skew data with the procedure above with the half patterned crystal in different positions determined by the rotation of $\pi/2$ of the crystal between each acquisition.

Table 2 shows the residual delays for each of the 4 positions of the crystal corresponding to the rotation of $\pi/2$. The time lag difference between the patterned half and the un-patterned half is not obvious. In order to enhance any subtle effect, we are summing the delays for each part of the crystal: patterned vs. non patterned. This is the total delay in the table 2. We have done also similar timing experience with a crystal with chamfered edges. In this experiment, the position of the edges was clearly seen on time stamps with contrasts of more than 10 time-stamps units. This is in sharp contrast also with what we have observed in section 3.1 in the number of photons. Thus we can conclude that the effect of photonics crystals on timing is subtle, not major.

While reading the table we can see although that the nanostructure part seem as an average to be always delayed in comparison to the naked part. To enhance any difference, we thus sum the time lag on each half of the crystal patterned or not for each of the 4 position tested, in order to try to put in evidence subtler effects. We are also calculating the mean value on the 8 dies on each side so that we can estimate the average time effect of the nanostructure.

Now a pattern appears: the patterned half is always slightly slower to deliver its first photons than the naked one. The difference is slight, within error bars for 3 distributions on 4, but it is always of the same sign. We would like to test the probability that the distributions are all identical and that the effect observed is not significant. We use the student test for each of the 4 series to define a p-value of the probability that the two distributions are identical. This gives the table below.

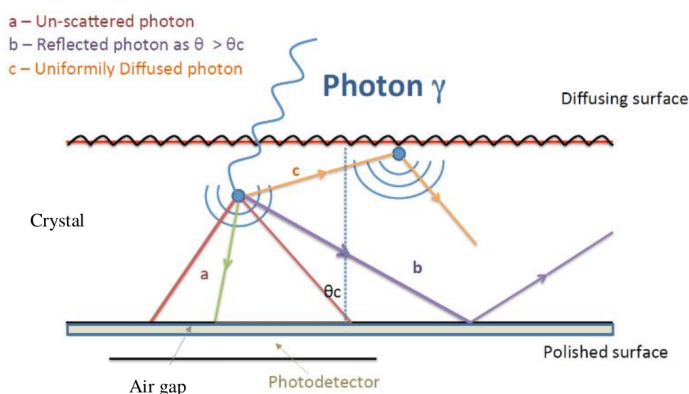
	<i>Series 1 (807)</i>	<i>Series 2 (806)</i>	<i>Series 3 (835)</i>	<i>Series 4 (959)</i>
t statistic	0.7138	2.1539	0.3839	0.3627
p-value	0.4956	0.0639	0.7070	0.7229

The probability that all four distributions are identical (i.e. that there is no time difference between naked crystal and nano-structured one) is the product of the probabilities of all 4 experiments.

Table 2. Delay skew table for each position of crystal (8 dies for textured, 8 dies for naked).

	Nanostructure	Naked crystal						
	5	13	4	2	4	2	1	7
	7	9	3	6	2	2	2	6
	7	9	4	0	2	1	4	5
	8	10	4	4	4	4	6	3
	8	7	3	1	4	3	5	4
	9	1	3	2	2	2	5	1
	8	0	4	0	0	1	4	3
	9	2	4	1	3	4	5	0
Total delay ¹	61	51	29	16	21	19	32	29
Mean	7.6	6.4	3.6	2	2.6	2.4	4	3.6
Standard deviation	0.9	4	0.5	1.5	1.1	0.9	1.2	1.9

¹: Unit = Philips DPC Time stamp = 19.5 ps.

**Figure 7.** Un-diffused photons and time stamps.

Thus the overall probability of the effect being not significant is 1.6%. We can exclude from this experiment any time gain bigger than 31ps related to the texturation as photonic crystal. The results obtained are marginally coherent with the absence of any timing effect: zero time lag. The best fit with data is obtained with a 0.9 Time stamp unit lag related to texturation, this translates in a 17ps delay on photon extraction.

As the index of LYSO is $n = 1.83$, this would translate into an average propagation length of scintillation photon enhanced by 2.8 mm on the nanostructured surface. The effect we are seeing is really tiny and at the limit of the experimental set-up. Unfortunately, the crystal was destroyed after the experiment. Assuming the effect observed is valid, could we find a physical explanation to this time lag?

3.4 Possible Interpretation of the slight delay related to the texturing

Once a scintillation event occurs in a crystal, photons are emitted in all directions. Because of the index mismatch between the crystal ($n = 1.83$) and the air gap ($n = 1$), there is a critical angle above which the photons are reflected back inside the scintillator (b). Thus, the first photons detected are the un-diffused ones (a), located inside a cone bounded by the critical angle. According to our timing acquisition procedure, the time stamps measured are mostly those of the un-diffused photons.

The effect of the photonic crystal patterning, as we have discussed earlier is to allow some photons above the critical angle (θ_c) to propagate outward and be detected directly, hence improving overall light extraction. At the same time the pattern shouldn't have much influence on photon extraction inside the critical angle. The photons ($\theta > \theta_c$) extracted at a higher angle will have a longer light path inside the crystal. Could this explain the slight delay observed?

4 Conclusions

Photonic crystals have been proposed as a way to improve light extraction on scintillating crystals [1]. They work by increasing the acceptance angle on the exit surface for photons trapped inside the crystal by total reflection. Photonic crystals thus increase photon escape probability.

A lot of work has been published on the enhancement of light extraction brought by photonic crystals. Little experimental results have been published on their effect on timing, although this parameter is very important for Time of Flight PET systems.

Here using a half patterned monolithic LYSO crystals, we are trying to overcome tricky calibration problems to measure both the impact of nano-texturation on light extraction but also on timing. Thus the crystal was rotated by a quarter of turn relative to the photo-detector during each set of measurements all other measurement variables being kept identical.

The pattern used for this experiment is a hexagonal network of TiO_2 cones of period 1000 nm, whose height averages 560 nm height and of a base diameter 300 nm. This pattern was deposited on the crystal using nano-imprint by Napa Technologies. The index of the TiO_2 was 2.15. The pattern covers only one half of the crystal and is clearly seen visually and thus easy to position on the Si-PM.

The impact on light extraction of the photonic crystal texturation is very strong as 30% of the light only escaped through the naked face vs 70% through the textured face.

The timing effect is much subtler. We are detecting an effect which is better explained by a slight time lag on photon extraction. The time lag if valid is less than 20 ps. This would in no way compromise the performance of a Time of Flight PET scanner built using photonic crystal as today commercial PET scanner time resolution is at best 250 ps. This effect is nevertheless perplexing as we were foreseeing a faster exit of photons on the textured face (5).

This may be explained by the larger acceptance angle of directly detected photons in the textured path. This could mean that some photons exiting the crystal through the textured part have in average a slightly longer light path in this experiment.

References

- [1] M. Kronberger, E. Auffray and P. Lecoq, *Probing the concepts of photonic crystals on scintillating materials*, *IEEE Trans. Nucl. Sci.* **55** (2008) 1102.
- [2] M. Kronberger, E. Auffray and P.R. Lecoq, *Improving light extraction from heavy inorganic scintillators by photonic crystals*, *IEEE Trans. Nucl. Sci.* **57** (2010) 2475.
- [3] P. Lecoq et al., *Factors influencing time resolution of scintillators and ways to improve them*, *IEEE Trans. Nucl. Sci.* **57** (2010) 2411.

- [4] A. Knapitsch et al., *Effects of photonic crystals on the light output of heavy inorganic scintillators*, *IEEE Trans. Nucl. Sci.* **60** (2013) 2322.
- [5] P. Lecoq, E. Auffray and A. Knapitsch, *How photonic crystals can improve the timing resolution of scintillators*, *IEEE Trans. Nucl. Sci.* **60** (2013) 1653.
- [6] G.A. Fornaro et al., *Study of the angular distribution of scintillation photons*, *IEEE Trans. Nucl. Sci.* **61** (2014) 456.
- [7] S. Zanettini et al., *Improved light extraction efficiency on 2 inches LYSO with nanopatterned TiO₂ photonic crystals*, posters at the *IEEE Nucl. Sci. Symp. Med. Imag. Conf.*, October 29–November 5, Strasbourg, France (2016).
- [8] T. Frach, G. Prescher, C. Degenhardt and B. Zwaans, *The digital silicon photomultiplier — System architecture and performance evaluation*, *IEEE Nucl. Sci. Symp. Med. Imag. Conf. Rec. (NSS/MIC)* (2010) 1722.
- [9] G. Borghi, V. Tabacchini and D.R. Schaart, *Towards monolithic scintillator based TOF-PET systems: practical methods for detector calibration and operation*, *Phys. Med. Biol.* **61** (2016) 4904.
- [10] A. Iltis et al., *Temporal imaging for PET: observation and precise localisation of photo-electric events inside a monolithic 20 mm LYSO plate with a Phillips digital Si-PM*, (2016).